Razavi SE., Sahebjam R., *BioImpacts,* 2014, 4(2), 89-94
doi: 10.5681/bi.2014.008
http://bi.tbzmed.ac.ir/

Research Article

Numerical simulation of the blood flow behavior in the circle of Willis

Seyyed Esmail Razavi*, Rana Sahebjam

School of Mechanical Engineering, University of Tabriz, Tabriz, Iran

Article info

Article History:
Received: 26 Aug. 2013
Revised: 18 Nov. 2013
Accepted: 30 Dec. 2013
ePublished: 30 June 2014

Keywords:
Circle of Willis
Newtonian fluid
non-Newtonian fluid
Navier-Stokes equations
FEM

Abstract

Introduction: This paper represents the numerical simulation of blood flow in the circle of Willis (CoW). Circle of Willis is responsible for the oxygenated blood distribution into the cerebral mass. To investigate the blood behavior, two Newtonian and non-Newtonian viscosity models were considered and the results were compared under steady state conditions.

Methods: Methodologically, the arterial geometry was obtained using 3D magnetic resonance angiography (MRA) data. The blood flow through the cerebral vasculature was considered to be steady and laminar, and the Galerkin's finite element method was applied to solve the systems of non-linear Navier-Stokes equations.

Results: Flow patterns including flow rates and shear rates were obtained through the simulation. The minimal magnitude of shear rates was much greater than 100 s^{-1} through the larger arteries; thus, the non-Newtonian blood viscosity tended to approach the constant limit of *infinite shear viscosity* through the CoW. So, in larger arteries the non-Newtonian nature of blood was less dominant and it would be treated as a Newtonian fluid. The only exception was the anterior communicating artery (ACoA) in which the blood flow showed different behavior for the Newtonian and non-Newtonian cases.

Conclusion: By comparing the results it was concluded that the Newtonian viscosity assumption of blood flow through the healthy, complete circle of Willis under the normal and steady conditions would be acceptably accurate.

Introduction

The circle of Willis is a ring-like arterial network in the base of the brain which is the main distributor of the nutrition and oxygenated blood throughout the cerebral mass. Cerebral circulation receives almost 15-20% of cardiac output. Blood is transmitted to the brain through two internal carotid arteries (ICAs) that contribute 80-85% of blood supply and two vertebral arteries (VAs) which join each other to form the basilar artery (BA). To follow the arterial path, middle and anterior cerebral arteries (MCAs and ACAs) and posterior cerebral arteries (PCAs) bifurcate in order to feed the whole cerebral portion.[1]

The Newtonian or non-Newtonian treatment of blood through the arterial networks can be a challenging research topic. Blood plasma that is mainly composed of water and some dissolved proteins and ions, totally exhibits a Newtonian fluid behavior.[2] The non-Newtonian nature of blood is due to the distinct behavior of erythrocytes under different shear rates. Blood viscosity tends to approach an *infinite shear viscosity* at shear rates greater than 100 s^{-1} due to the erythrocytes' deformation. When the shear rates are less than 100 s^{-1}, the blood cells aggregate to form rouleaux, then the shear thinning nature of blood becomes dominant and the effective viscosity increases. In smaller blood vessels such as communicating arteries, or large vessels where the flow has been reduced by a stenosis or occlusion, the shear rates are less than 100 s^{-1} and hence the viscosity increases.[3] These manners are also affected by a parameter termed *Hematocrit*. Hematocrit indicates the volume percentage of blood cells over the total blood volume. As the hematocrit increases, the viscosity rises nonlinearly.[4]

Regarding the cerebral arteries, there have been some researches performed on the blood flow in the CoW. Primarily, 1D structural model with Poiseuille flow assumption was applied. The works of Hillen *et al.* and Cassot *et al.* treated the flow in the circle of Willis as 1D unsteady pulsatile flow in straight elastic walled tubes.[5-7] The ability of the CoW in providing collateral flow in response to an occlusion of the ICA was studied by Viedma *et al.*[8] Alastruey *et al.* presented a model of 1D equations of pressure and flow wave propagation in compliant arteries.[9] They showed there is a continuous blood flow towards the brain during all the cardiac cycles. Afterwards, 2D models improved the geometry definition. Ferrandez *et al.* treated the flow in the CoW as unsteady non-pulsatile in

***Corresponding author:** Seyed Esmail Razavi, Email: razavi@tabrizu.ac.ir

a 2D rigid walled structure.[10,11] They studied the transient response of blood flux in efferent arteries as a result of afferent pressure changes.

To achieve more realistic results, 3D models were considered in some papers. The works of Cebral *et al.* illustrated the patient-specific models treating the flow as unsteady pulsatile in 3D rigid and distensible models.[12,13] The models were generated from time-of-flight magnetic resonance imaging (TOF-MRI) data, and a finite element scheme was applied to solve the equations. Kim *et al.* studied the blood flow in the carotid and cerebral arteries and the Navier-Stokes equations were applied with the gravity effects taken into account.[14] Moore *et al.* applied 3D Navier-stokes equations using the finite volume method to investigate the effects of 3D CoW anatomical variation on the cerebral hemodynamic.[15,16] The blood flow was modeled as unsteady, incompressible and viscous. An autoregulation mechanism had been developed and three pathological conditions were explored. The results proved the vital role of the autoregulation mechanism in adjusting the efferent blood flows in response to the afferent pressure changes. Zuleger *et al.* simulated the non-Newtonian blood flow through the circle of Willis using 3D TOF-MR data for geometry acquiring and showed the areas having high averaged wall shear stress gradients (AWSSG) correspond to the most common locations of aneurismal formation.[17]

In this paper, we investigated the blood flow to find out whether it treats as a Newtonian or non-Newtonian fluid through the circle of Willis for the first time. The three-dimensional Navier-Stokes equations were solved using the Galerkin's FEM. The flow is normally laminar through the cerebral vasculature and the pulsatile nature of blood flow was also ignored. Thus the assumptions of steady laminar flow were applied and the flow characteristics were discussed.

Materials and methods

Anatomical modeling

The model geometry has been obtained using the magnetic resonance imaging data combined with computer-aided design (CAD) software. Applying the method, three orthogonal plans taken from a single MRA scan were imported to the CAD package CATIA. First, the wireframe was created with 3D splines; afterwards, the arteries' diameters were applied and the model was completed by creating and smoothing the junctions. Fig. 1 demonstrates the model generating steps using the generative shape design order in CATIA. The completed geometry is illustrated in Fig. 2.

Table 1 shows the geometric dimensions taken from Moore *et al.*[15] These magnitudes were obtained from a population study of MRA scans. The diameters were measured using an in-house software package by which the various slices from a TOF MRA scan could be read and by dragging a cursor between points of interest, the measurements would be obtained. For the complete CoW, 13 cases were examined and the standard deviations were obtained. Their model included the VAs in addition to the others, thus the BA-B1, BA-B2 imply the diameters of different parts of the VAs and the BA. In this work, the mean values were used to create the model.

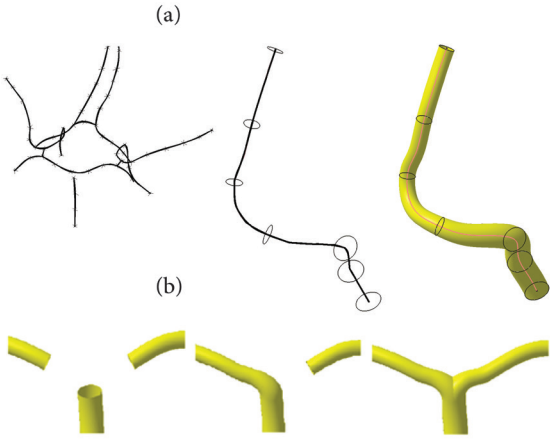

Fig. 1. (a) The projected curve created into a 3D sketch with points and the process of creating the arterial walls (b) the procedure of creating junctions when the parent and daughter arteries are of similar diameter.

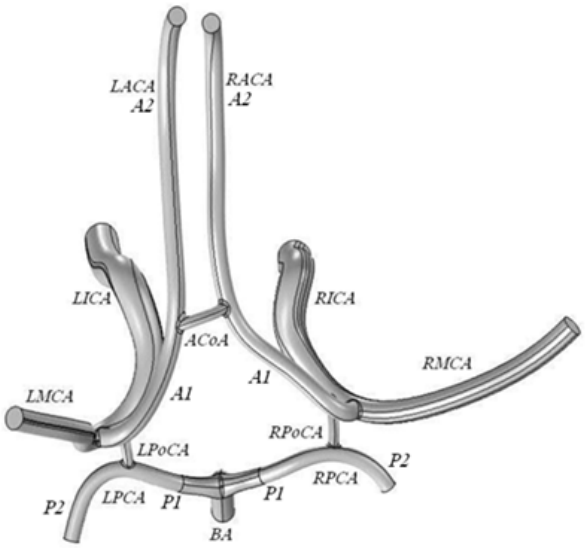

Fig. 2. Complete Circle of Willis geometry

Table 1. Complete Circle of Willis measurements

Artery	Diameter (mm)	Standard deviation (mm)
ACA-A1	2.33	0.22
ACA-A2	2.4	0.31
MCA	2.86	0.17
PCA-P1	2.13	0.25
PCA-P2	2.10	0.21
ACoA	1.47	0.17
PCoA	1.45	0.31
BA-B1	3.17	0.51
BA-B2	3.29	0.44
ICA	4.72	0.26

The images concern the MRA scan of a healthy mature man which had a rather complete circle structure. This method helped us to get more authentic physiological approximation to the cerebral vasculature. Of course, there are some finer details which may be lost during the modeling, but compared to the total dimension these topological features have minor effects in the main efferent blood supply under the normal conditions. An important point to be declared is the boundaries in terminal locations, which should be far enough away from the arterial connections in order to reach fully developed velocity profiles. Considering the arterial path to the cerebral network, the blood flow becomes fully developed after passing the short laminar entrance length (x= 0.06*D*Re_x)[18] and reaches the fully developed condition before entering the CoW. The parabolic velocity profile ($u = u_{max}(1-(\frac{r}{R})^2)$) would be an appropriate assumption to state the velocity distribution through the circle of Willis arteries.

Governing equations

In the current work, blood flow through the circle of Willis was modeled as steady, incompressible and viscous. Therefore, the governing equations to be solved are the continuity equation:

$$\nabla.\vec{V} = 0 \quad (1)$$

The momentum equation is shown in Eq. (2)

$$\rho[\frac{\partial \vec{V}}{\partial t} + (\vec{V}.\nabla)\vec{V}] = \nabla.[-pI + \tau] + F \quad (2)$$

where $\vec{V}$, p and ρ indicate velocity vector, pressure vector and the fluid density, respectively. F represents any additional momentum sink to be incorporated.[15] τ, the deviatoric stress tensor which is related to the strain rate tensor is usually expressed as

$$\tau = \mu\dot{\gamma} \quad (3)$$

where μ is the fluid viscosity and $\dot{\gamma}$ is the strain rate vector.[19] For the incompressible flow, the strain rate tensor is defined as

$$\dot{\gamma} = 2D = \nabla\vec{V} + \nabla\vec{V}^T \quad (4)$$

where D is the rate of deformation tensor. Unlike the constant viscosity for a Newtonian fluid, the viscosity of a non-Newtonian fluid is a function of the second invariant of the rate of deformation tensor, $|\dot{\gamma}|$ and is given by

$$\mu = \mu(|\dot{\gamma}|) \quad (5)$$

in which

$$|\dot{\gamma}| = \sqrt{2tr(D^2)} \quad (6)$$

To account for the non-Newtonian nature of blood, the Carreau model has been applied,

$$\frac{\mu - \mu_\infty}{\mu_0 - \mu_\infty} = [1 + (\lambda\dot{\gamma})^2]^{\frac{(n-1)}{2}} \quad (7)$$

where μ_0 and μ_∞ are the zero and infinite shear viscosities respectively taken as 0.056 and 0.00345 Pa s. The remaining parameters λ and n were taken as 3.313 s and 0.3568, respectively.[20] A 0.00345 Pa s viscosity was considered for the Newtonian case.

Numerical method and boundary conditions

The numerical modeling of an incompressible viscous flow requires the solution of the Navier-Stokes and the continuity equations. The flow simulation was performed by the COMSOL software, in which the mesh was generated using tetrahedral elements. Also, the Galerkin's FEM was adopted for discretization and solving the equations, thus the following set of non-linear differential equations was obtained: [21]

$$L\vec{V} = 0 \quad (8)$$

$$M\vec{V} + [S(\vec{V}) + N(\vec{V})]\vec{V} + L^T p = f \quad (9)$$

where $\vec{V}$ and p are columns containing the velocity components and pressure values, M the mass matrix, $S(\vec{V})$ the diffusion matrix, $N(\vec{V})$ the non-linear convection matrix, L the divergence matrix, and f are columns containing the body and boundary forces.

In the present study, systemic and venus pressures at the inlets and outlets of the afferent and efferent arteries were applied as the boundary conditions. Neglecting the pulsatile nature of afferent blood pressure, an inlet pressure equal to 100 mmHg and a 4 mmHg outlet blood pressure were specified as the inlet and outlet boundary conditions, respectively.[15] Considering the arterial wall, it was decided to treat it as a rigid structure and impose the no-slip condition.

Results

The streamlines, shear rates and the flow rates were obtained for the arterial network of the circle of Willis over two Newtonian and non-Newtonian states. Fig. 3 illustrates the streamlines through the cerebral arteries. As seen, there is almost no flow through the ACoA for both cases. There are some other uncolored regions that indicate the missing streamlines through the larger arteries in order to get clear illustrations. The flow rates are shown in Fig. 4 for both Newtonian and non-Newtonian cases. The comparison of results clarifies that there are minor negligible differences between them, verifying the fact that in larger arteries the non-Newtonian nature of blood is less dominant and it would be treated as a Newtonian fluid. A point to be declared is that the Newtonian results are rather greater than the non-Newtonian ones. Regarding the non-Newtonian case, there are some locations where the effective blood viscosity exceeds the infinite shear viscosity (Fig. 5). It implies a further resistance against the flow in these sections and lower flow rates through the arteries in non-Newtonian case.

The geometric model of the presented work demonstrates a noticeable difference between two MCAs' branches.

This topological feature causes a dramatic difference between the flow characteristics through the right middle cerebral artery (RMCA) and left middle cerebral artery (LMCA). Compared with the previous works,[14,15] the RMCA's structure is more alike to the usual anatomy. The abnormality of LMCA's structure is because of its intense slope which causes a higher flow rate passing through the artery (Fig. 3, Fig. 4). As the result, the Reynolds number calculated for this branch is about 900, indicating the probability of the turbulent flow, separation and the embolus formation. An embolus is frequently a blood clot, detached from a blood vessel wall which travels in the bloodstream until it becomes wedged in an artery, cutting off its blood supply and probably rising the risk of ischemic stroke.

The axial velocity profiles in two sections are obtained and shown in Fig . 5. The parabolic velocity distribution was set to describe the flow characteristics. The sections were chosen in two MCA branches, far enough away from the arterial connections to reach the fully developed condition. It is clear that the differences were small and negligible.

As seen in Fig. 3 there is almost no flow through the ACoA under normal condition for both cases. This causes considerably low shear rates through the ACoA and a high effective viscosity for the non-Newtonian case (Fig. 6, 7). Excluding the communicating arteries (especially the ACoA), the minimal amount of the shear rates through the arterial walls was much higher than 100 s^{-1}, so the blood viscosity tended to approach a constant limit. That is, both Newtonian and non-Newtonian assumptions

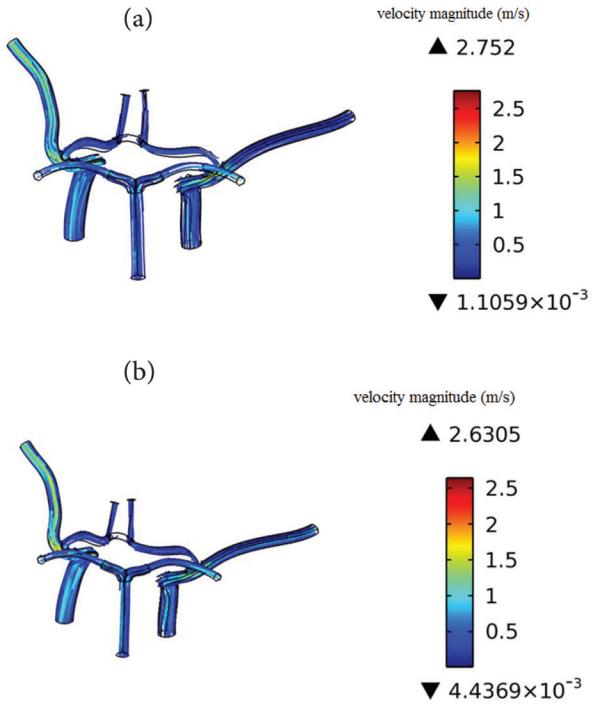

Fig. 3. Streamlines through the circle of Willis for the (a) Newtonian, and (b) non-Newtonian cases

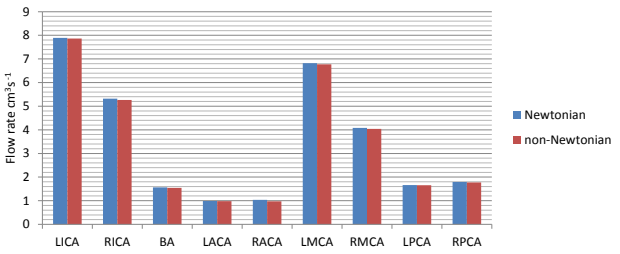

Fig. 4. Flow rates through the cerebral arteries under normal condition. There are minor differences between the Newtonian and non-Newtonian results.

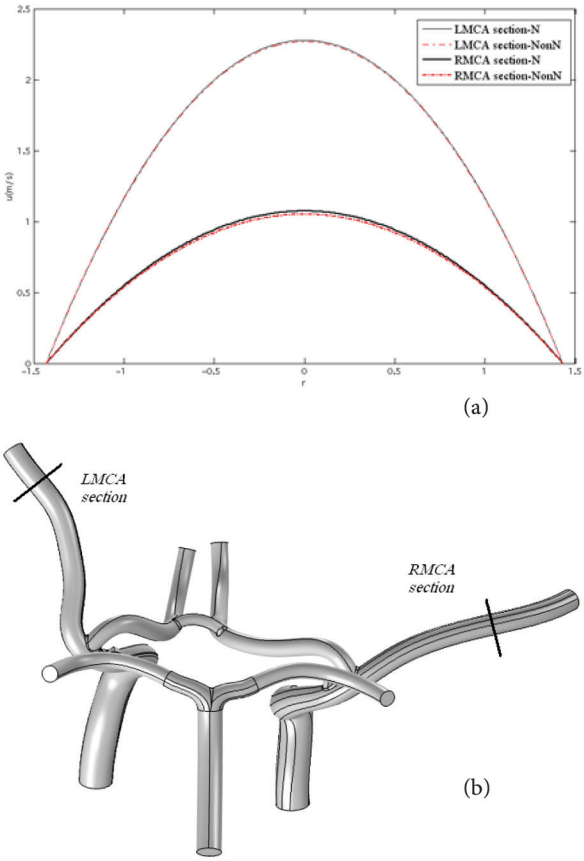

Fig. 5. (a) Velocity profiles in two sections through the RMCA and LMCA and (b) the section sites

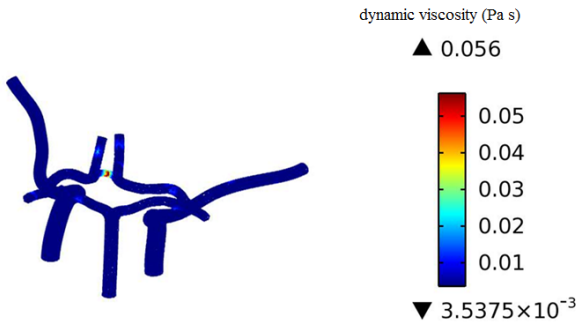

Fig. 6. Some locations of effective viscosity, exceeding the infinite shear viscosity

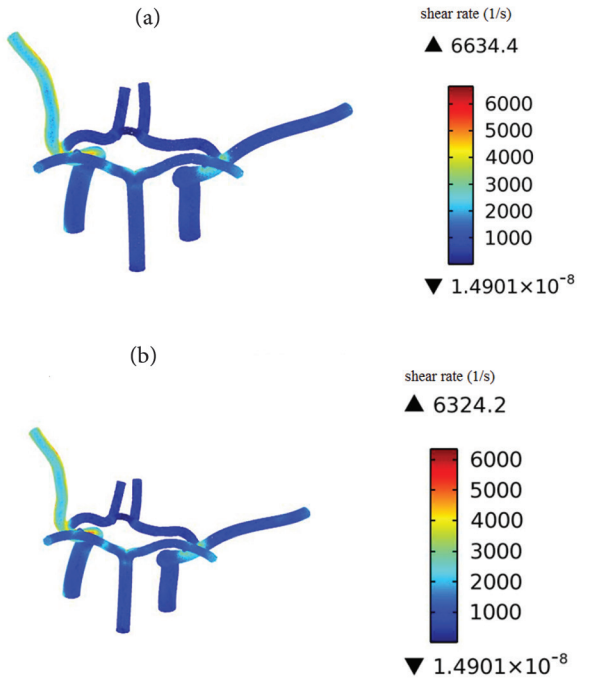

Fig. 7. Shear rates through the cerebral arteries for the (a) Newtonian and (b) non-Newtonian cases

resulted in similar outcomes; so it could be concluded that the blood flow through the healthy, complete circle of Willis would be treated as a Newtonian fluid under the normal and steady conditions.

Discussion

The non-Newtonian nature of blood is mainly a function of the hematocrit and the flow shear rate. In this work the effects of blood's shear thinning behavior on the flow properties through the cerebral vasculature was studied. The model was based on a complete healthy anatomy. The normal steady conditions were considered.

The results showed that the shear thinning properties of blood causes Newtonian fluid behavior through the CoW. The exception was the ACoA, showing considerably distinct behaviors under two conditions. To consider the larger arteries, there were minor differences between Newtonian and non-Newtonian results. As a result the Newtonian viscosity model would be a reasonable approximation to describe the blood flow characteristics through the larger arteries as well as the cerebral arteries (the larger arteries include those in which the shear rates are much greater than 100 s^{-1}).

Conclusion

As a consequence it would be declared that the blood flow through the healthy, complete circle of Willis would be treated as a Newtonian fluid under the normal and steady conditions.

The studies concerning the distensible walls and unsteady conditions require further works. Furthermore, the clinical data and experimental studies would help us to get more authentic results in order to achieve the patient-specific flow characteristics, which is an essential point in planning the treatments.

Ethical Issues

There is none to be declared.

Competing interests

Authors declare no competing interests.

References

1. Devault K, Gremaud PA, Novak V, Olufsen MS, Vernieres G, Zhao P. Blood flow in the circle of Willis: Modeling and calibration. *Multiscale Model Simul* **2008**; 7: 888-909.
2. Prokop V, Kozel K. Numerical simulation of Newtonian and non-Newtonian flows in bypass. *Mathematics and Computers in Simulation* **2010**; 80: 1725-1733.
3. Wang Sh, Chen J, Ding G, Lu G, Zhang X. Non-Newtonian computational hemodynamics in two patient-specific cerebral aneurysms with daughter saccules. *Journal of Hydrodynamics* **2010**; 22: 639-646.
4. Cinar Y, Demir G, Pac M, Cinar AB. Effects of hematocrit on blood pressure via hyperviscosity. *Am J Hypertens* **1999**; 12: 739-743.
5. Hillen B, Gaasbeek T, Hoogstranet HW. A mathematical model of the flow in the posterior communicating arteries. *J Biomech***1982**; 15: 441-449.
6. Hillen B, Hoogstraten HW, Post L. A mathematical model of the flow in the circle of Willis. *J Biomech* **1986**; 19: 187-194.
7. Cassot F, Zagzoule M, Marc-Vergnes JP. Hemodynamic role of the circle of willis in stenoses of internal carotid arteries. An analytical solution of a linear model. *J Biomech* **2000**; 33: 395–405.
8. 8. Viedma A, Jimenz Ortiz C, Marco V. Extended Willis circle model to explain clinical observations in periorbital arterial flow. *J Biomech* **1997**; 30: 265-272.
9. Alastruey J, Parker KH, Peiro J, Byrd SM, Sherwin SJ. Modeling the circle of Willis to assess the effects of anatomical variations and occlusion on cerebral flows. *J Biomech* **2007**; 40:1794-1805.
10. Ferrandez A, David T, Brown MD. Numerical models of autoregulation and blood flow in the cerebral circulation. *Compute Methods Biomech Biomed Engin* **2002**; 5: 7-19.
11. David T, Brown M, Ferrandez A. Auto-regulation and blood flow in the cerebral circulation. *International Journal of Methods in Fluids* **2003**; 43: 701-713.
12. Cebral J, Lohner P, Yim J, Burgess JE. Blood flow predictions during neuro-surgery and carotid artery stenting. *International Journal of Bioelectromagnetism* **2001**; 3: 1-12.
13. Cebral JR, Castro MA, Soto O, Lohner R, Alperin N. Blood flow models of the circle of Willis from

magnetic resonance data. *Journal of Engineering Mathematics* **2003**; 47:369-386.
14. Kim CSS, Kiris C, Kwak D, David T. Numerical simulation of local blood flow in the carotid and cerebral arteries under altered gravity. *Journal of Biomechanical Engineering-Transactions of the ASME* **2006**; 128: 194-202.
15. Moore S, David T, Chase JG, Arnold J, Fink J. 3D models of blood flow in the cerebral vasculature. *J Biomech* **2006**; 39: 1454-1463.
16. David T, Moore S. Modeling perfusion in the cerebral vasculature. *Mechanical Engineering and Physics* **2008**; 30: 1227-1245.
17. Zuleger DI, Poulikakos D, Valavanis A, Kollias SS. Combining magnetic resonance measurements with numerical simulations- Extracting blood flow physiology information relevant to the investigation of intracranial aneurysm in the circle of Willis. *InternationalJournal of Heat and Fluid Flow* **2010**; 31: 1032-1039.
18. White FM. *Fluid Mechanics*. 5th edition. New York: McGraw-Hill;**2005.**
19. Wei G, Ru-xun L, Ya-li D. Numerical investigation on non-Newtonian flows through double constrictions by an unstructured finite volume method. *Journal of Hydrodynamics* **2009**; 21: 622-632.
20. Arjmandi-Tash O, Razavi SE, Zanbouri R. Possibility of artherosclerosis in an arterial bifurcation model. *BioImpacts* **2011**; 1: 225-228.
21. Gijsen FJH, van de Vosse FN, Janssen JD. The influence of the non-Newtonian properties of blood on the flow in large arteries: steady flow in a carotid bifurcation model. *J Biomech* **1999**; 32: 601-608.